Assessment of turbulence hybrid models with transition modeling for the simulation of massively separated flows

F.Miralles[1], B.Sauvage[3], S.Wornom[1], B.Koobus[1], A.Dervieux[2,3]

[1]IMAG, Université de Montpellier, France,
[2] Société LEMMA, Sophia-Antipolis, France
[3]INRIA Sophia-Antipolis, France

22nd Computational Fluids Conference,
April 25-28, 2023, Cannes

Introduction

Motivation of this work

- Development of accurate and efficient tools for the simulation of acoustic radiation generated by rotating machines (NORMA ANR research project).

Figure – Helicopter, wind turbines and taxi drone

- Need for turbulence models which
  a are accurate for massively separated flows at high Reynolds numbers,
  b able to take into account transitional boundary layers,
  c introduce little dissipation in order to perform well in aeroacoustic computations.

Introduction

Background : main models

- RANS not suited for accurate predictions for flows with massive separation and for aeroacoustic problems.

Figure – Mach field of RANS simulation over a NACA0018.

- LES computationally too expensive, particularly in the near wall regions and with increasing Reynolds numbers.

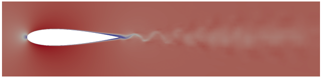

Figure – Mach field of LES simulation over a NACA0018.

- Hybrid RANS-LES models can be good candidate for aeroacoustic simulations characterized by massive separations, a special attention should be paid to the choice of the LES model, the RANS component and the blending strategy.

Purpose of this work

Assessment of different hybrid strategies for the simulation of a circular cylinder flow from sub-critical to super-critical regime, in order to capture drag crisis phenomenon.

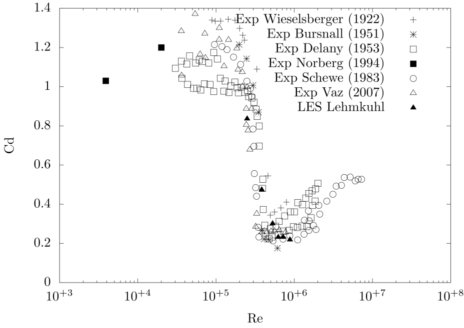

URANS component : baseline turbulence model

- Based in this work, either on the RANS $k-\varepsilon$ of Goldberg [1] and $k-\varepsilon-\gamma$ model of Akther [2] can be written briefly :

$$\frac{\partial W}{\partial t} + \nabla \cdot F_c(W) + \nabla \cdot F_v(W) + \nabla \cdot F_v^{RANS}(W) = \tau^{RANS}(W)$$

- RANS $k-\varepsilon$ Goldberg [3] and a new $k-\varepsilon-\gamma$ based on Akther's model :

$$\tau^{k-\varepsilon}(W_h) = \left(\overbrace{0}^{\rho}, \overbrace{\mathbf{0}}^{\rho \mathbf{u}}, \overbrace{0}^{\rho E}, \overbrace{P_k - D_k}^{\rho k}, \overbrace{(C_1 \tau : \nabla \mathbf{u} - C_2 \rho \varepsilon + E) T^{-1}}^{\rho \varepsilon} \right)$$

$$\tau^{k-\varepsilon-\gamma}(W_h) = \left(\overbrace{0}^{\rho}, \overbrace{\mathbf{0}}^{\rho \mathbf{u}}, \overbrace{0}^{\rho E}, \overbrace{\gamma P_k - \max(\gamma, 0.1) D_k}^{\rho k}, \overbrace{(C_1 \tau : \nabla \mathbf{u} - C_2 \rho \varepsilon + E) T^{-1}}^{\rho \varepsilon} \right)$$

- The transition onset is given by Abu-Ghannam's correlation

$$Re_{\theta,S} = 163 + \exp(6.91 - Tu)$$

1. U. Goldberg, O. Peroomian et S. Chakravarthy. "A wall-distance-free $k-\varepsilon$ model with Enhanced Near-Wall Treatment". In : *Journal of Fluids Engineering* 120 (1998), p. 457-462.
2. Most. Nasrin Akhter, Mohammad Ali et Ken ichi Funazaki. "Numerical Simulation of Heat Transfer Coefficient on Turbine Blade using Intermittency Factor Equation". In : *Procedia Engineering* 105 (2015). The 6th BSME International Conference on Thermal Engineering, p. 495-503. issn : 1877-7058.
3. U. Goldberg, O. Peroomian et S. Chakravarthy. "A wall-distance-free $k-\varepsilon$ model with Enhanced Near-Wall Treatment". In : *Journal of Fluids Engineering* 120 (1998), p. 457-462.

LES component : Dynamic Variational Multi Scale

- VMS Principle

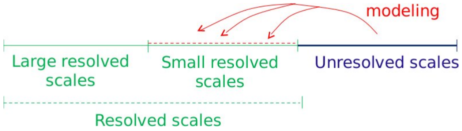

Our VMS[4] uses 2 embedded grids in order to dissipate solely the numerical scales which are the smallest represented by the mesh and not the larger ones.

$$\frac{\partial W}{\partial t} + \nabla \cdot F_c(W) + \nabla \cdot F_v(W) + \nabla \cdot F_v^{VMS}(W^{small\ scales}) = 0$$

- Dynamic VMS[5] is a combination of VMS with Germano-type dynamic algorithm adapting in space and time the SGS coefficient :

$$C_s \longrightarrow C_s(\mathbf{x}, t)$$

4. B.Koobus et C. Farhat. "A variational multiscale method for the large eddy simulation of compressible turbulent flows on unstructured meshes—application to vortex shedding". In : *Computer Methods in Applied Mechanics and Engineering* 193.15 (2004). Recent Advances in Stabilized and Multiscale Finite Element Methods, p. 1367-1383.

5. C. Moussaed et al. "Impact of dynamic subgrid-scale modeling in variational multiscale large-eddy simulation of bluff-body flows". In : *Acta Mechanica* 225 (2014), p. 3309-3323.

Hybrid approach in a finite volume/ finite element framework

$$\left(\frac{\partial W_h}{\partial t}, \chi_i\right) + (\nabla \cdot F_c(W_h), \chi_i) = (\nabla \cdot F_d(W_h), \phi_i)$$
$$+ \theta \left(\tau^C(W_h), \phi_i\right) + (1-\theta)\left(\tau^{DVMS}(W_h^{small\ scales}), \phi_i^{small\ scales}\right)$$

- ⋆ $\tau^C \in \{\tau^{RANS}, \tau^{DDES}\}$
- ⋆ Blending : $\theta = 1 - f_d \times (1 - \overline{\theta})$; $\overline{\theta} = \tanh\left(\left(\frac{\Delta}{k^{3/2}}\varepsilon\right)^2\right)$,
- ⋆ $f_d = f_{ddes}$ or $f_d = f_{geo} = \exp\left(-\frac{1}{\epsilon}\min(d - \delta_0, 0)^2\right)$

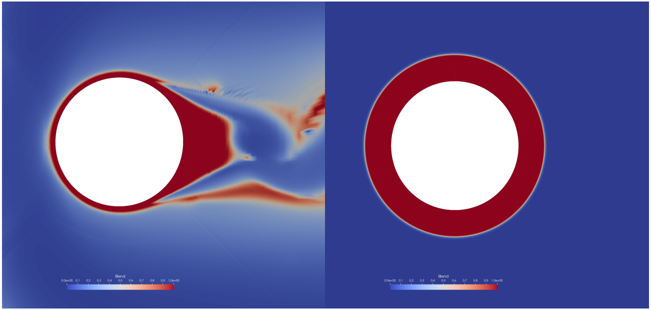

Figure – Hybrid URANS DVMS blending surface.

Set up

- Simulation set up :
  - Mach number : 0.1 (subsonic flow)
  - reference pressure : 101300 $[\mathrm{N/m^2}]$
  - density : 1.225 $[\mathrm{kg/m^3}]$
  - Wall boundaries conditions :

$$\begin{aligned} \mathbf{u} = \mathbf{0}, &\quad \nabla T \cdot \mathbf{n} = 0, \\ k - \varepsilon : &\quad k = 0,\ \varepsilon = (\nabla \sqrt{k}) \cdot \mathbf{n}, \\ \gamma : &\quad \nabla \gamma \cdot \mathbf{n} = 0. \end{aligned}$$

  - The mesh is radial with minimal mesh size such that $y_w^+ \simeq 1$ for $Re = 10^6$ (610K Nodes).

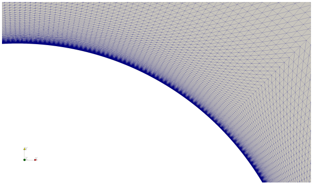

Figure – Computational grid zoom close to the surface.

Circular cylinder Re = 20,000 : sub-critical regime

Figure – $k - \varepsilon - \gamma$/DVMS flow at Reynolds 20K, Q-Criterion field using velocity color scale

	$\overline{C}_d$	$\lvert\overline{C}_L\rvert$	C_l'	$-\overline{C}_{pb}$	θ_{sep}	St
Present simulation Re=20, 000						
$k-\varepsilon$/DVMS	1.10	0.00	0.60	0.85	85	0.22
$k-\varepsilon-\gamma$/DVMS	1.22	0.00	0.48	1.19	89	0.21
Simulation						
LES of Aradag [6]	1.20	-	-	1.25	-	-
VMS-LES of Wornom [7]	1.27	-	0.60	1.09	86	0.19
Experiments						
Norberg [8]	1.16	-	0.46	1.19	-	0.19
Lim [9]	1.19	-	-	1.09	-	-

Table – Bulk coefficients of the flow around a circular cylinder at Reynolds number 20,000 (sub-critical regime). $\overline{C}_d$ holds for the mean drag coefficient, $|\overline{C}_l|$ denotes the absolute value of the mean lift coefficient, C_l' is the root mean square of the lift coefficient, $\overline{C}_{p_b}$ is the value of the mean base pressure coefficient, θ_{sep} is the mean separation angle, and St is the vortex shedding frequency. $k-\varepsilon$/DVMS holds for the hybrid model without intermittency modeling, and $k-\varepsilon-\gamma$/DVMS is the present intermittency-based hybrid model.

6. S.ARADAG. "Unsteady turbulent vortex structure downstream of a three dimensional cylinder". In : *Isi Bilimi Ve Teknigi Dergisi/ Journal of Thermal Science and Technology* 29 (jan. 2009).

7. S. Wornom et al. "Variational multiscale large-eddy simulations of the flow past a circular cylinder : Reynolds number effects". In : *Computers and Fluids* 47.1 (2011), p. 44-50. issn : 0045-7930.

8. C Norberg. "Pressure Forces on a Circular Cylinder in Cross Flow, IUTAM Symposium on Bluff Body Wakes, Dynamics and Instabilities". In : sept. 1992. isbn : 978-3-662-00416-6 ; C. Norberg. "Fluctuating lift on a circular cylinder : review and new measurements". In : *Journal of Fluids and Structures* 17.1 (2003), p. 57-96. issn : 0889-9746.

9. H.Lim et S.J. Lee. "Flow Control of Circular Cylinders with Longitudinal Grooved Surfaces". In : *AIAA Journal* 40.10 (2002), p. 2027-2036.

■ Pressure coefficient (Exp from Norberg [10])

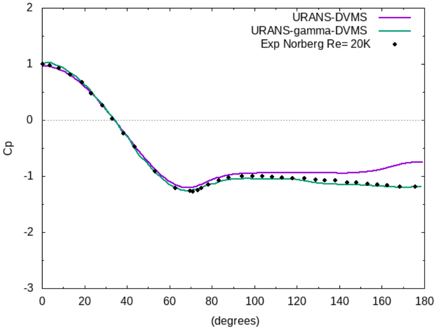

Figure – Flow past a cylinder at Reynolds number 20,000 (sub-critical regime) : distribution over the cylinder surface of the mean pressure coefficient obtained with the present intermittency-based hybrid model compared to experimental data

10. C Norberg. "Pressure Forces on a Circular Cylinder in Cross Flow, IUTAM Symposium on Bluff Body Wakes, Dynamics and Instabilities". In : sept. 1992. isbn : 978-3-662-00416-6.

Circular cylinder Re = 250K : critical regime

Figure – $k - \varepsilon - \gamma$/DVMS flow at Reynolds 250K, Q-Criterion field using velocity color scale

Name	$\overline{C}_d$	$\lvert\overline{C_L}\rvert$	C_l'	$-\overline{C}_{pb}$	St
Present simulation Re=2.5 $\times 10^5$					
$k-\varepsilon$/DVMS	0.61	0.00	0.31	0.70	0.30
$k-\varepsilon-\gamma$/DVMS	0.86	0.15	0.65	0.87	0.20
Simulation					
LES of Lehmkuhl et al. [11]	0.83	0.9	0.49	0.99	0.24
LES of Yeon at al. [12]	0.56	0.09	0.12	0.44	0.19
Experiments					
Schewe [13]	1.00	-	0.18	-	0.20

Table – Bulk coefficients of the flow around a circular cylinder at Reynolds number 2.5×10^5 (critical regime). Same symbols as in Table 1

11. I. Rodríguez et al. "On the flow past a circular cylinder from critical to super-critical Reynolds numbers : Wake topology and vortex shedding". In : *International Journal of Heat and Fluid Flow* 55 (2015), p. 91-103. issn : 0142-727X.

12. S.M. Yeon, J. Yang et F. Stern. "Large-eddy simulation of the flow past a circular cylinder at sub- to super-critical Reynolds numbers". In : *Applied Ocean Research* 59 (2016), p. 663-675. issn : 0141-1187.

13. G. Schewe. "On the force fluctuations acting on a circular cylinder in crossflow from subcritical up to transcritical Reynolds numbers". In : *Journal of Fluid Mechanics* 133 (1995), p. 265-285.

Pressure coefficient (Exp from Achenbach [14])

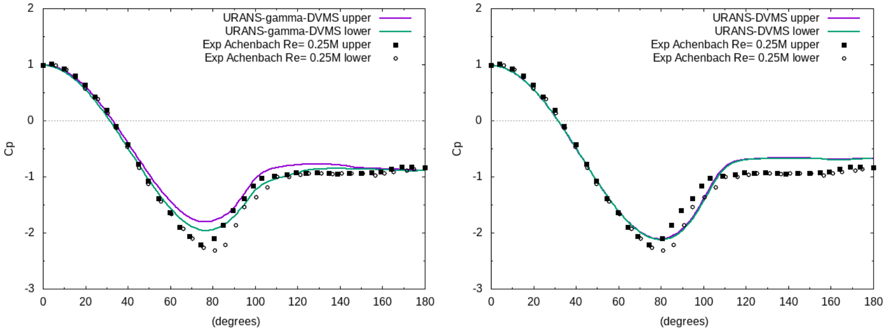

Figure – Flow past a cylinder at Reynolds number 2.5×10^5 (critical regime) : distribution over the upper part (purple) and the lower part (green) of the cylinder surface of the mean pressure coefficient obtained with the present intermittency-based hybrid model (left) and its counterpart without transition (right), compared to experimental data (Achenbach).

14. E. Achenbach et E. Heinecke. "On vortex shedding from smooth and rough cylinders in the range of Reynolds numbers 6×103 to 5×106". In : *Journal of Fluid Mechanics* 109 (1981), 239–251.

Circular cylinder Re = 1M : super-critical flow

Figure – $k - \varepsilon - \gamma$/DVMS flow at Reynolds 1M, Q-Criterion field using velocity color scale

	$\overline{C}_d$	$\lvert\overline{C}_L\rvert$	C'_l	$-\overline{C}_{pb}$	θ_{sep}	St
Present simulation Re=10^6						
$k-\varepsilon$/DVMS	0.54	0.03	0.30	0.50	110	0.34
$k-\varepsilon-\gamma$/DVMS	0.28	0.03	0.04	0.25	128	0.50
Simulation						
LES of Kim et al. [15]	0.27	-	0.12	0.28	108	-
LES of Catalano et al. [16]	0.31	-	-	0.32	-	0.35
Experiments						
Schewe [17]	0.22	-	0.02	-	-	0.44
Gölling [18]	0.22	-	-	-	130	0.12/0.47
Zdravkovich [19]	0.2-0.4	-	0.1-0.15	0.2-0.34	-	0.18/0.50

Table – Bulk coefficients of the flow around a circular cylinder at Reynolds number 10^6 (super-critical regime). Same symbols as in Table 1

15. S.E. Kim et M. Srinivasa. "Prediction of Unsteady Loading on a Circular Cylinder in High Reynolds Number Flows Using Large Eddy Simulation". In : t. 3. Jan. 2005.

16. P. Catalano et al. "Numerical simulation of the flow around a circular cylinder at high Reynolds numbers". In : *International Journal of Heat and Fluid Flow* 24.4 (2003), p. 463-469. issn : 0142-727X.

17. G. Schewe. "On the force fluctuations acting on a circular cylinder in crossflow from subcritical up to transcritical Reynolds number". In : *Journal of Fluid Mechanics* 133 (août 1983), p. 265 -285.

18. B. Gölling. "Experimental investigations of separating boundary-layer flow from circular cylinder at Reynolds numbers from 10^5 up to 10^7". In : 2006, p. 455-462.

19. M.M. Zdravkovich. *Flow Around Circular Cylinders : Volume I : Fundamentals*. Flow Around Circular Cylinders : A Comprehensive Guide Through Flow Phenomena, Experiments, Applications, Mathematical Models, and Computer Simulations. OUP Oxford, 1997.

■ Pressure coefficient (Exp from Warschauer[20])

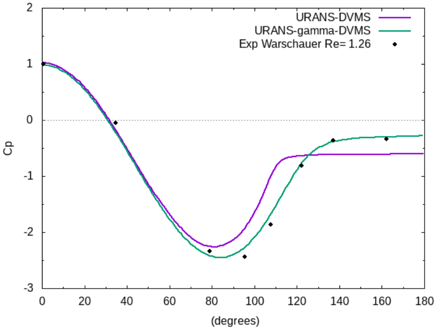

Figure – Flow past a cylinder at Reynolds number 10^6 (super-critical regime) : distribution over the cylinder surface of the mean pressure coefficient obtained with the present intermittency-based hybrid model compared to experimental data.

20. J.A. Leene K.A.Warschauer. "Experiments on mean and fluctuating pressures of circular cylinders at cross flow at very high Reynolds numbers". In : 1971, p. 305-315.

Vorticity fields

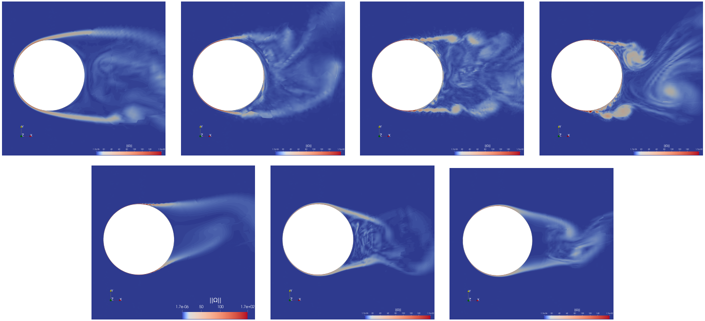

Figure – Instantaneous vorticity magnitude in spanwise-cross section for various Reynolds numbers from sub-critical to super-critical flow regimes (from left to right, top then bottom : Re=3900, Re=20,000, Re=10^5, Re=2.5×10^5, Re=3.8×10^5, Re=7.2×10^5, Re=10^6).

Drag crisis and increase in Strouhal number

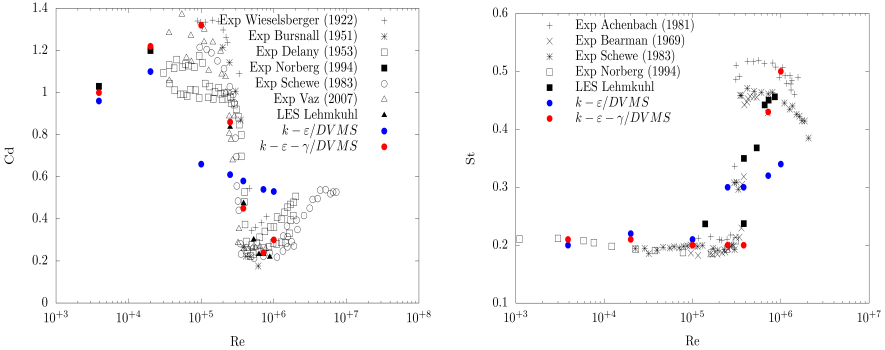

Figure – Impact of the intermittency model (in red) on the drag crisis and Strouhal number prediction, in contrast with the same hybrid model without intermittency modeling (in blue).

Conclusion and perspective

- Investigation of a hybrid method which combines an intermittency-based RANS model and a DVMS approach.
- Application to circular cylinder flows at various regimes.
- Bulk coefficients and important phenomena (like drag crisis and increase in Strouhal number) are properly predicted.
- Significant improvement brought by the intermittency-based hybrid method compared to its non-transitional counterpart.
- Suitability of the hybrid approach at high Reynolds numbers using relatively coarse grids.
- Usability of the proposed hybrid model over a wide range of Reynolds numbers, including moderate ones.

Aerodynamic and aeroacoustic simulation of complex flows in rotating machines and over three-dimensional airfoils in incidence.

Appendix VMS

- VMS formulation [21]

$$\left(\frac{\partial W_h}{\partial t},\chi_i\right) + (\nabla\cdot F_c(W_h),\chi_i) = (\nabla\cdot F_d(W_h),\phi_i) + \left(\tau^{DVMS}(W_h),\phi_i^{'}\right). \qquad (1)$$

- VMS closure term with dynamics coefficients $\mathcal{C}_{model} = \mathcal{C}_{model}(\mathbf{x},t)$ and $Pr_t = Pr_t(\mathbf{x},t)$

$$\left(\tau^{DVMS}(W_h),\phi_i^{\prime}\right) = \left(0, \mathbf{M}_S(W_h,\phi_h^{'}), M_H(W_h,\phi_h^{'}), 0, 0\right)$$

where :

$$\mathbf{M}_S(W_h,\phi_i^{\prime}) = \sum_{T\in\Omega_h}\int_T \underbrace{\overline{\rho}(C_S\Delta)^2|S|}_{\mu_{sgs}} P\nabla\phi_i^{\prime} d\mathbf{x}, \quad P = 2S - \tfrac{2}{3}Tr(S)Id$$

$$M_H(W_h,\phi_i^{\prime}) = \sum_{T\in\Omega_h}\int_T \frac{C_p}{Pr_t}\underbrace{\overline{\rho}(C_S\Delta)^2|S|}_{\mu_{sgs}} \nabla T^{\prime}\cdot\nabla\phi_i^{\prime} d\mathbf{x}, \quad \Delta = \left(\int_T d\mathbf{x}\right)^{1/3}$$

and $\phi_h^{'} = \phi_h - \overline{\phi_h}$ where $\overline{\phi_h}$ is computed from macro cells.

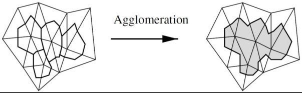

21. C. Farhat, A. Rajasekharan et B. Koobus. "A dynamic variational multiscale method for large eddy simulations on unstructured meshes". In : *Computer Methods in Applied Mechanics and Engineering* 195.13 (2006). A Tribute to Thomas J.R. Hughes on the Occasion of his 60th Birthday, p. 1667-1691. issn : 0045-7825. doi : https://doi.org/10.1016/j.cma.2005.05.045. url : https://www.sciencedirect.com/science/article/pii/S0045782505003014.